Figure S1

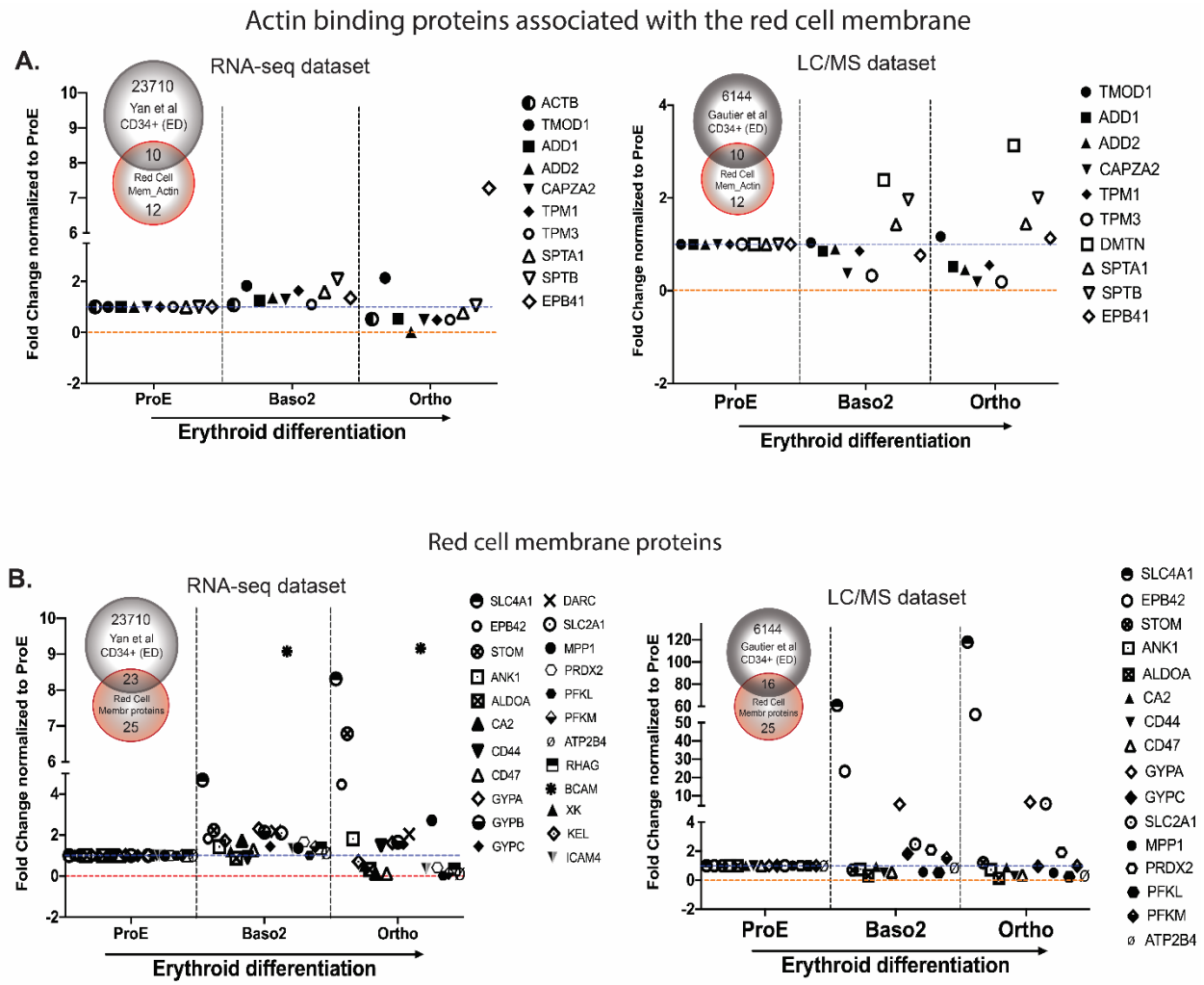

Figure S1: Database mining for known ABPs associated with the mature red cell membrane skeleton, and other red cell membrane proteins, as benchmarking for our search strategy for novel ABPs/NFs. Using our curated list of ABPs associated with the red cell membrane skeleton and other known red cell membrane-associated proteins (Appendix Table S1B), changes in mRNA expression levels were assessed from proerythroblast (ProE), basophilic erythroblast (Baso2), and orthochromatic erythroblast (OrthoE) stages. (A) Within the mature red cell membrane skeleton proteins dataset, most of the genes did not display an increase in mRNA expression at the OrthoE stage with respect to the ProE stage. The proteomics (LC-MS) dataset confirmed well-known expression changes for various red cell membrane skeleton proteins including tropomodulin (TMOD1), DMTN, and spectrins (SPTA1, SPTB). (B) Various known red cell transmembrane and membrane-associated proteins were found to be transcriptionally and translationally upregulated at the OrthoE stage (SLC4A1, EPB42). This demonstrated that our database mining methodology provided appropriate benchmarking for analyses of a test group of other ABPs/NFs (Figure 1).

Figure S2

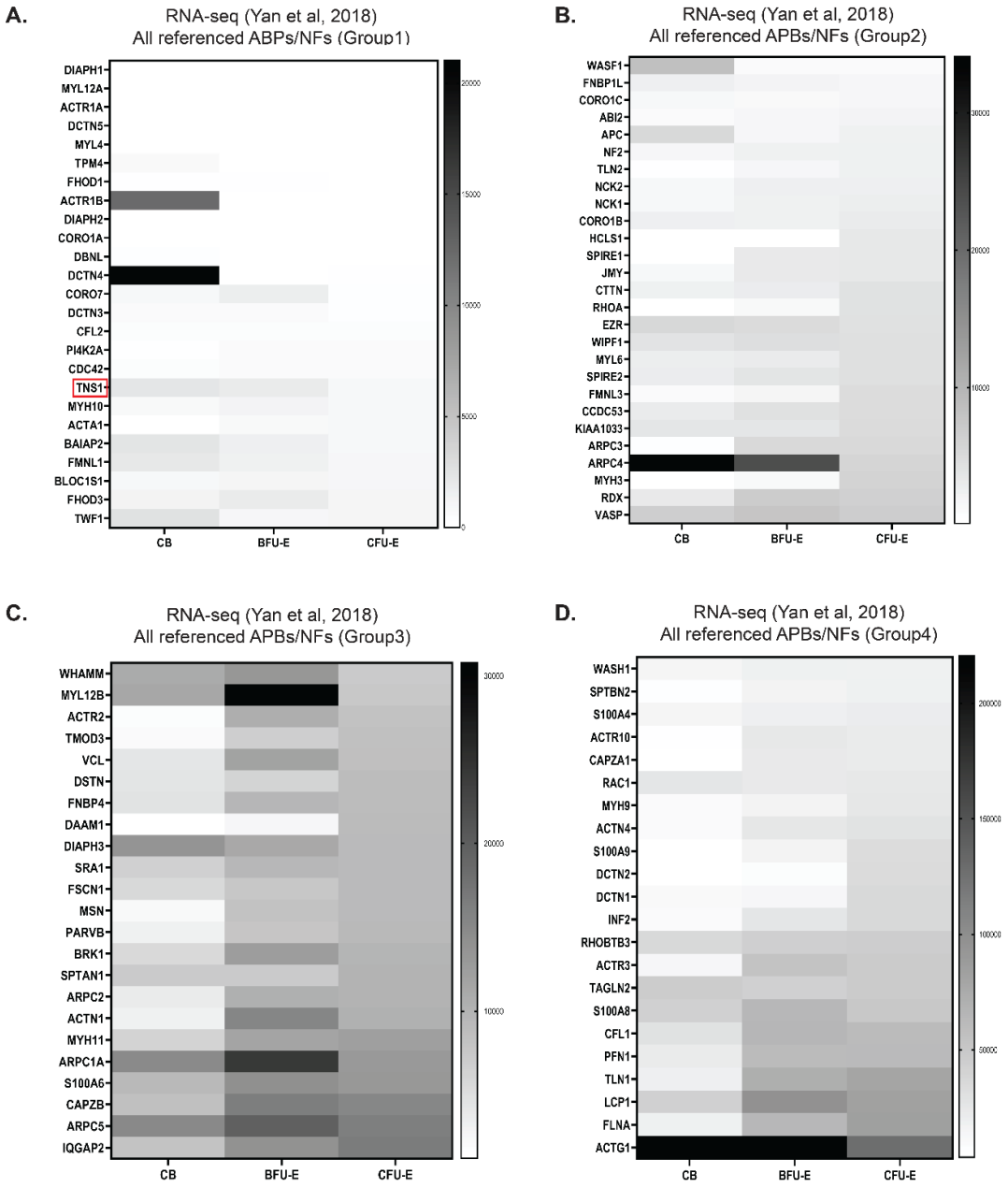

Figure S2: Analysis of expression levels for 97 ABP/NF hits from the RNA-seq dataset reveals *TNS1* mRNA levels remain low during early stages of erythroid differentiation. The RNA-seq dataset hits were unbiasedly clustered arbitrarily into 4 separate groups for optimal visualization via heatmap on GraphPad Prism v10 (cluster 1 = 25 genes, cluster 2 = 27 genes, cluster 3 = 23 genes, cluster 4 = 22 genes). All clusters display raw counts from early stages of erythroid differentiation (CB = Cord Blood; BFU-E = Burst-Forming Unit-Erythroid; CFU-E = Colony-Forming Unit-Erythroid), with higher expression indicated by a darker rectangle. The majority of the 97 ABP/NF hits, including TNS1 (red box), showed no significant change in mRNA expression at these early stages of erythroid differentiation.

Figure S3

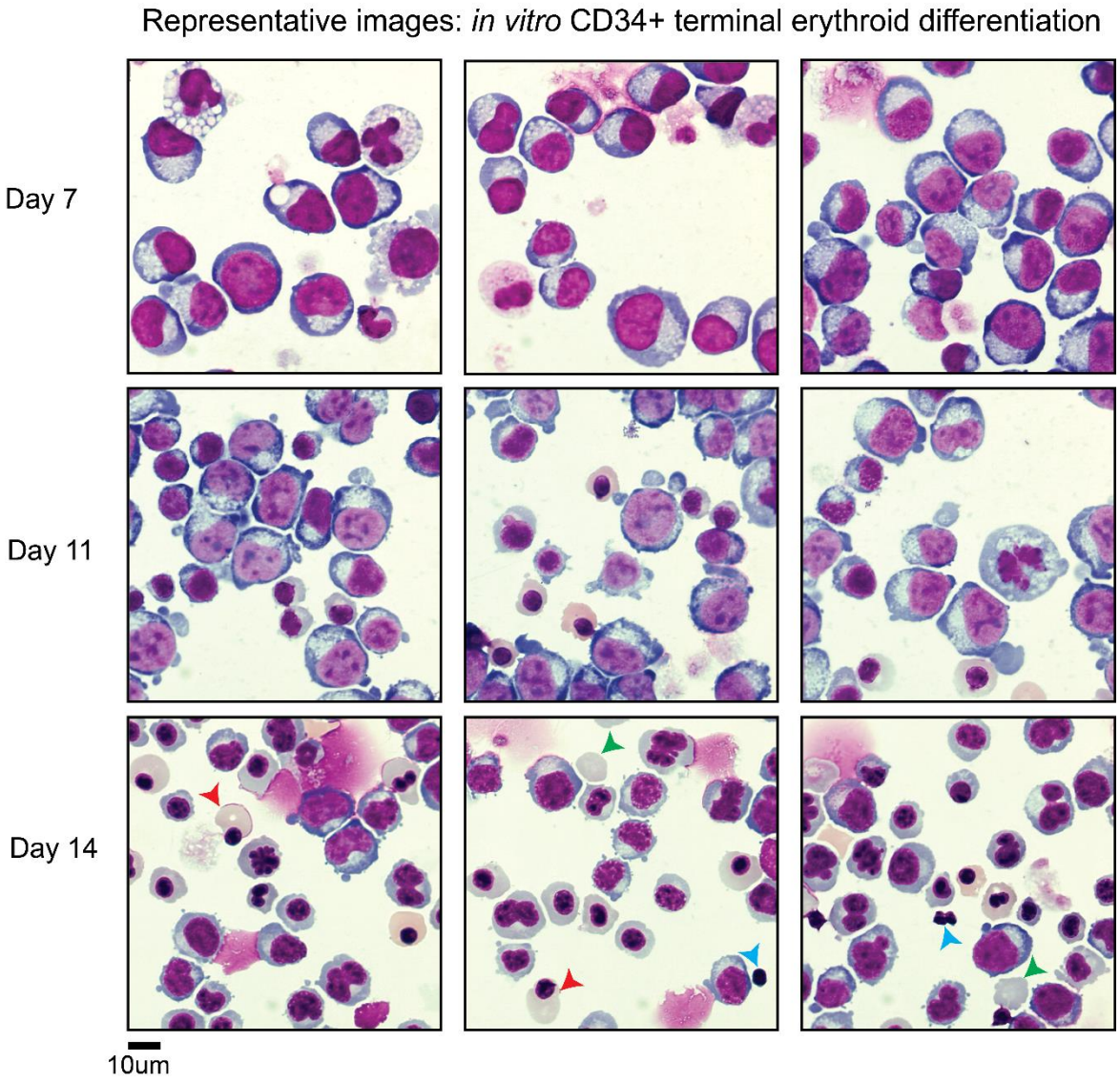

Figure S3: Morphological analysis confirms terminal erythroid differentiation of human CD34+ cells in vitro. Representative images of Wright-Giemsa stained CD34+ cells at days 7, 11, and 14 during in vitro erythroid differentiation show expected morphological changes of maturing erythroblasts. Scale bar, 10 µm. Day 7 cultures are primarily composed of larger cells with uncondensed nuclei. By day 11, smaller cells with condensed nuclei either centrally located or polarized to one side of the cell can be seen. Although these cultures remain heterogeneous, by day 14, cells begin to enucleate (red arrows) resulting in reticulocytes (green arrow) and pyrenocytes (blue arrow).

Figure S4

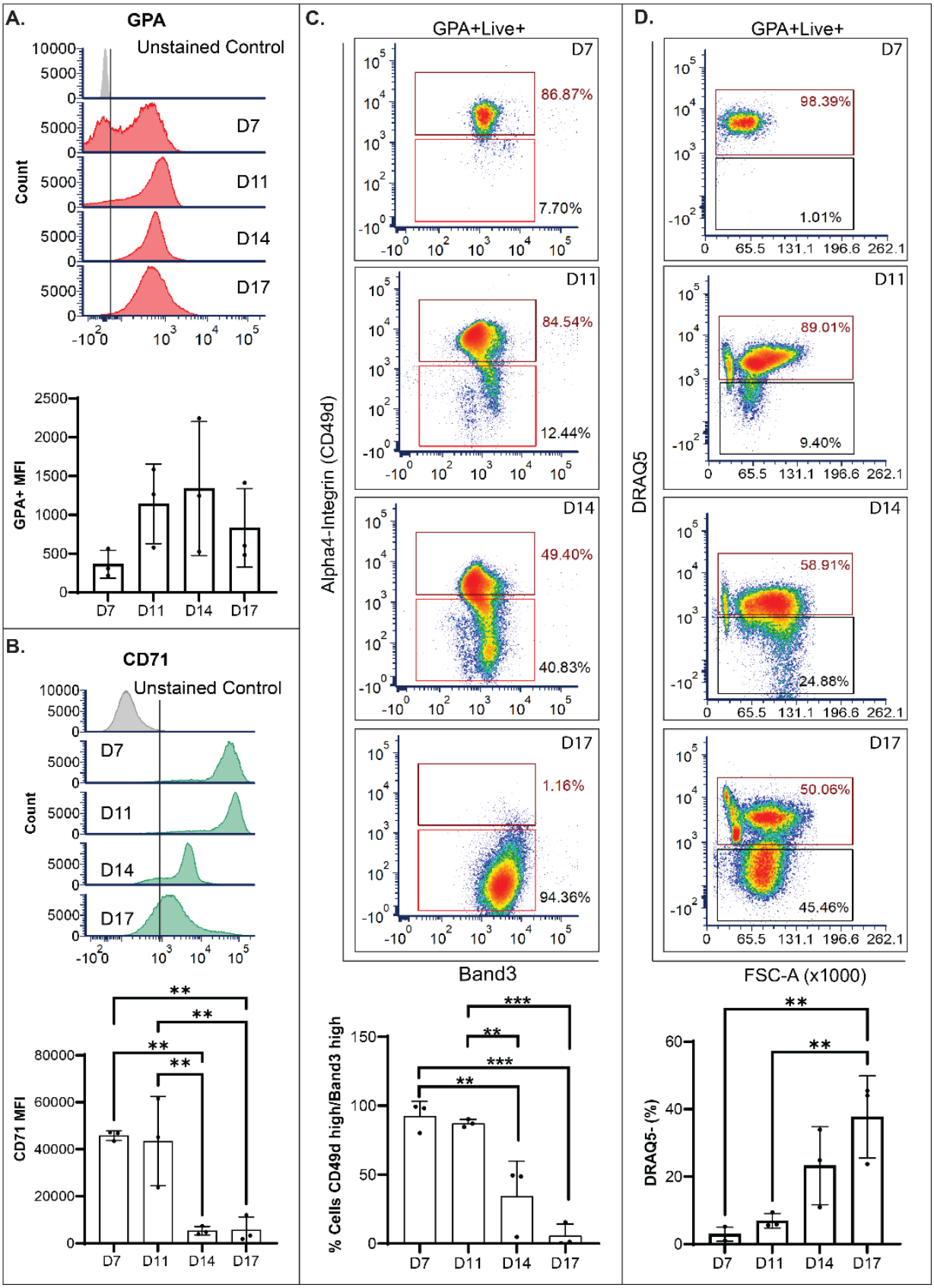

Figure S4: Flow cytometric analysis of human CD34+ cells in erythroid cultures confirms surface marker characteristics of terminally differentiating erythroblasts. (A-B) Histograms and quantification of mean fluorescence intensity for glycophorin A (GPA) and transferrin receptor (CD71) levels in differentiating (control) CD34+ cells. Unstained cells used as a gating control. Only live cells were analyzed. © Live GPA-positive cells analyzed for CD49d (α4-integrin) and band3 expression. Gates set for CD49d-high, band3-hi (maroon), and graphed as a change in percentage population across 3 biological replicates. (D) Live GPA-positive cells analyzed for enucleation efficiency using DRAQ5 dye, gated for DRAQ5-positive (maroon) and DRAQ5-negative (black gate) cells and graphed as a change in percentage of population for DRAQ5 negative across 3 biological replicates. Values are mean ± SD from 6 individual erythroid cultures. *$p<0.05$; **$p<0.01$; ***$p<0.001$.

Figure S5

A.

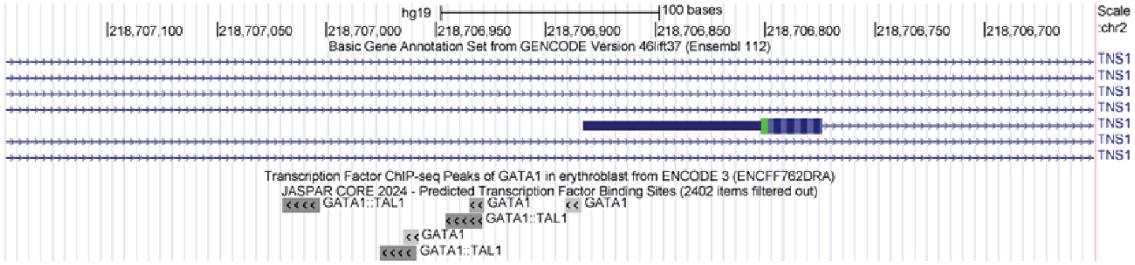

B.

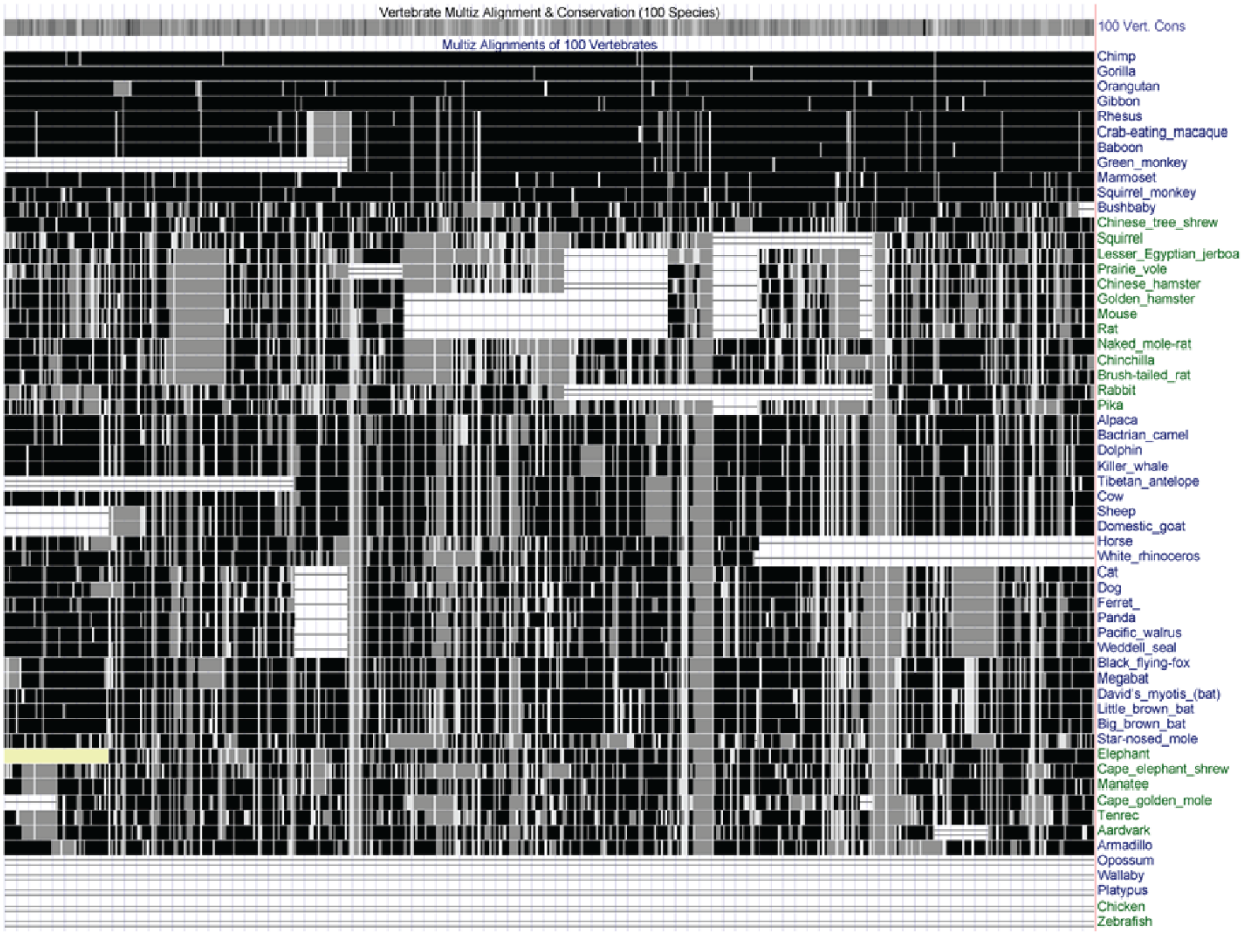

Figure S5: Conservation at the TNS1 locus across vertebrate species. (A) The region encoding the human erythroid exon 1E and 5' flanking putative promoter region is shown. Exon 1E is shown as a blue bar. The location of the initiator methionine of the erythroid TNS1 peptide (eTNS1) in exon 1E is shown in green. Candidate transcription factor binding sites for GATA-1 and TAL-1 are indicated below. (B) Multi-alignment analysis of 100 vertebrates reveals strong conservation among primates. Regions deleted from genomes of individual species are shown in white.

Figure S6

A.

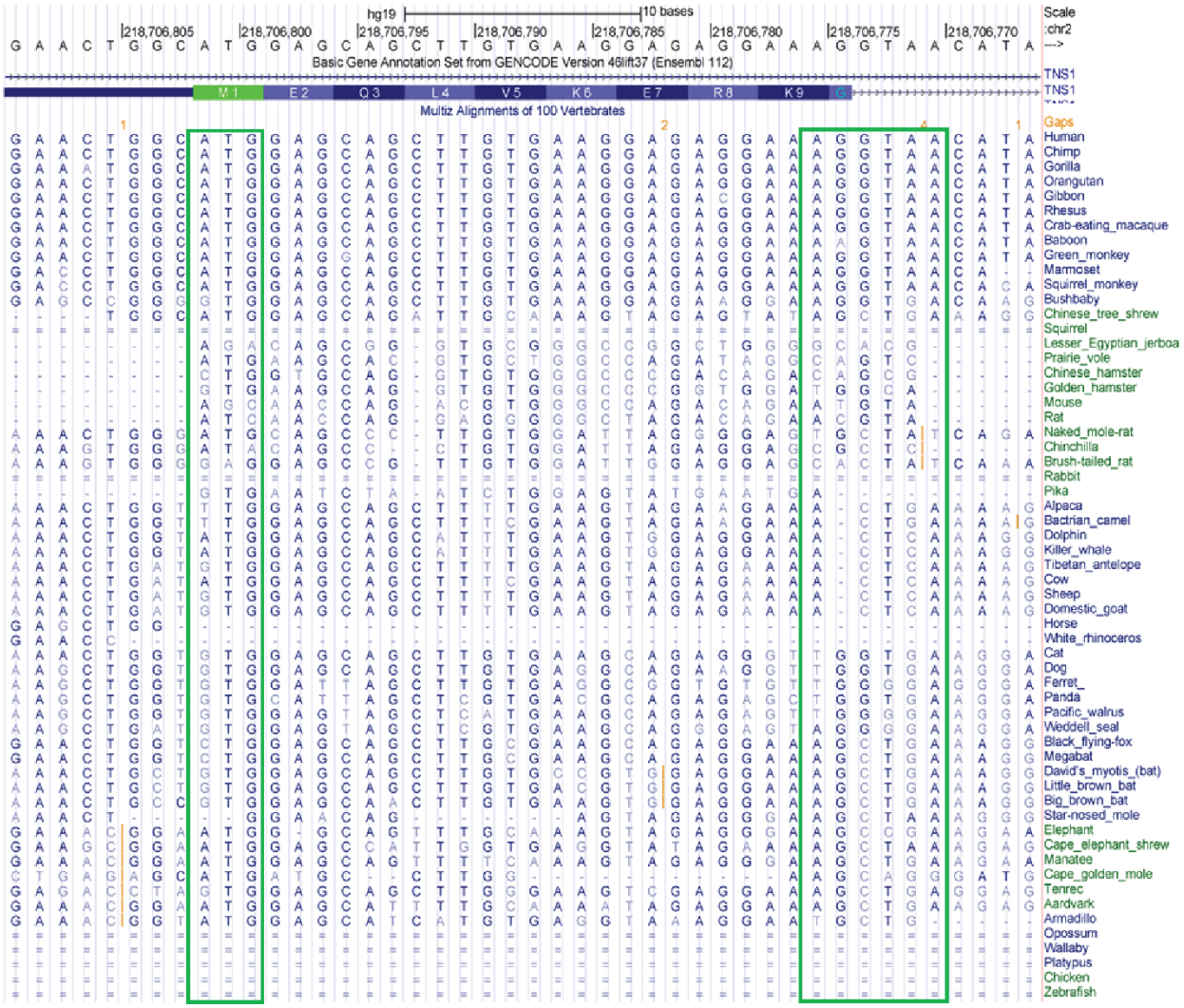

Figure S6: Nucleotide-level analysis at the TNS1 locus across vertebrate species. The region encoding the human erythroid exon 1E is shown. The location of the initiator methionine for the erythroid TNS1 protein (eTNS1) in exon 1E is indicated in green. There is strong conservation of the 5' untranslated region, initiator methionine, coding region, and 5' donor splice site among primates in multi-alignment analysis of 100 vertebrates. Other species lack the upstream 5' untranslated region, the "A" of the initiator methionine "ATG" and/or the 5' donor splice site consensus sequence, AG:gttaa.

Figure S7

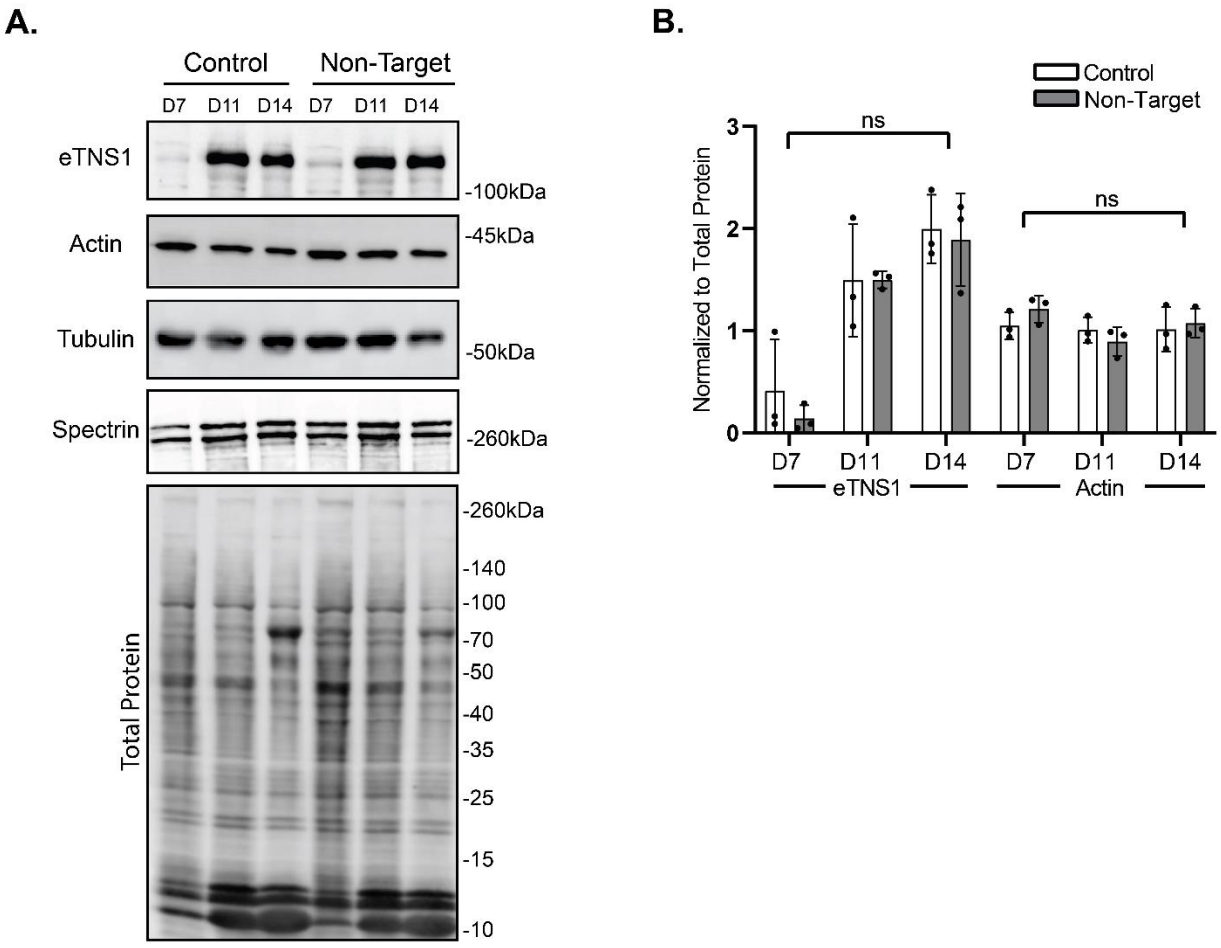

Figure S7: Introduction of CRISPR/Cas9 RNP complexes containing non-target crRNA had no effects on eTNS1, total actin, α-tubulin, or erythroid spectrin protein expression. (A) Representative Western blots of eTNS1, total actin, α-tubulin, (α1β1)-spectrin, and total protein during in vitro terminal erythroid differentiation of CD34+ cells in non-transfected control cultures compared to non-target cultures. 15 µg protein loaded per lane. (B) Quantification of eTNS1 and total actin in control compared to non-target cells, normalized to total protein. Band intensities were analyzed by ImageJ. Values are means ± SD from 3 individual CD34+ erythroid cultures.

Figure S8

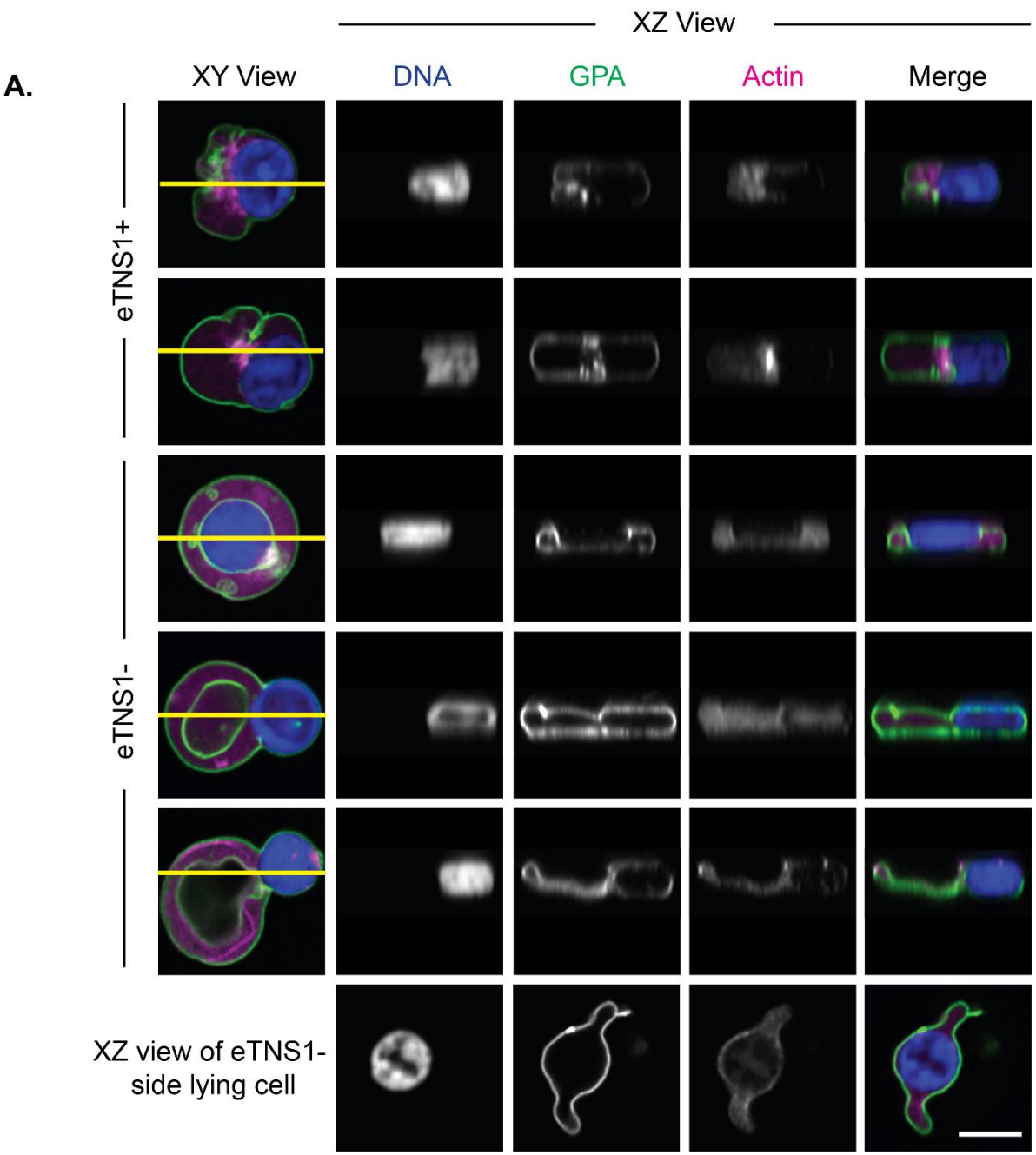

Figure S8: CRISPR/Cas9 knockout of eTNS1 results in human erythroblasts stuck in process of nuclear expulsion, with altered morphology resembling a biconcave cell. (A) Single optical sections from Airyscan Z-stacks of polarized and enucleating eTNS1+ and eTNS1- erythroblasts. eTNS1- cell shapes appeared to resemble biconcave discs (GPA in white), despite the retention of the nucleus in the cell. Z-sections of cells were used to construct an XY side view of each cell at the location of the yellow line. Scale bar, 5 µm.

Supplemental Table 1: List of known ABPs and NFs used in data mining strategy to identify ABPs/NFs increased during terminal erythroid differentiation. (A) 135 known ABPs and NFs were identified from multiple studies and compiled into groups based on gene description and actin-associated function. Associated Genbank IDs are provided. Database mining was conducted by comparing this curated list of 135 ABPs/NFs to RNA-seq and proteomics (LC-MS) datasets. (B) For reference controls, 12 known ABPs associated with the red cell membrane skeleton and 25 red cell transmembrane and membrane-associated proteins were identified and were also catalogued for analysis. Data mining of our curated list was benchmarked via comparing the expression profiles of these known red cell membrane ABPs and other red cell membrane proteins.

Supplemental Table 2: RNA-seq and LC-M/S profiles of compiled ABPs and NFs. Database mining was conducted by comparing a curated ABP/NF gene list to RNA-seq and LC-M/S hits from Yan et al, 2018 and Gautier et al, 2016 respectively. (A) RNA-seq hits were converted to linear scale for 97 ABP/NFs. The BasoE and OrthoE expression levels were normalized to ProE as shown. (B) RNA-seq hits were also analyzed for expression at the CB, BFU-E and CFU-E stage. The 97 RNA-seq hits were additionally clustered based on expression (low to high, Cluster 1-4) levels based on the CFU-E stage. TNS1 was found in cluster 1. (C) 49 LC-M/S hits were compiled from data mining and certain hits with missing values (BRK1, WIPF1, FMNL1, SPTBN2) were not considered for profiling in Figure 1D.